Clinical Radiology 77 (2022) 840–847

Contents lists available at ScienceDirect

Clinical Radiology

journal homepage: www.clinicalradiologyonline.net

Monitoring mild cognitive impairment of workers exposed to occupational aluminium based on quantitative susceptibility mapping

Z.Y. Zhang [a,†], H.R. Jiang [a,†], X.R. Sun [a], X.C. Wang [b], Q. Niu [c], H.X. Meng [c], J.F. Du [b], G.Q. Yang [b], H. Zhang [b,**], Y. Tan [b,*]

[a] *College of Medical Imaging, Shanxi Medical University, Taiyuan 030001, Shanxi Province, China*
[b] *Department of Radiology, First Clinical Medical Hospital, Shanxi Medical University, 85 Jiefang South Road, Taiyuan 030001, Shanxi Province, China*
[c] *School of Public Health, Shanxi Medical University, Taiyuan 030001, Shanxi Province, China*

ARTICLE INFORMATION

Article history:
Received 13 November 2021
Received in revised form
28 May 2022
Accepted 8 June 2022

AIM: To investigate the diagnostic value of quantitative susceptibility mapping (QSM) in mild cognitive impairment (MCI) of aluminium (Al) workers.

MATERIALS AND METHODS: The basic data of 53 workers in an Al factory were collected and divided into the MCI group and normal control (NC) group by Montreal Cognitive Assessment (MoCA) scores. All participants were tested for plasma Al concentration and had magnetic resonance imaging (MRI). The QSM values of many areas of the brain were delineated and measured. Independent two-sample *t*-tests or non-parametric tests were used to compare the parameter values between the two groups. Spearman's correlation analysis was performed between QSM values, MoCA scores, and plasma Al concentration. The receiver operating characteristic curve and z test were performed to assess diagnostic efficacy and the best parameter.

RESULTS: There was no difference in age and educational level. Plasma Al concentration of the MCI group was higher than that of NC group (p=0.057). QSM values of the left hippocampus, left dentate nucleus, right substantia nigra, and left putamen in MCI group were higher than that of NC group (p<0.05), and the left hippocampus had the best diagnostic efficacy. QSM values correlated negatively with MoCA scores. No correlation was found between QSM values and plasma Al concentration (p>0.05).

CONCLUSION: QSM might be a neuroimaging marker for the diagnosis of MCI. The left hippocampus showed the best diagnostic efficacy. Plasma Al concentration of the MCI group was higher than that of the NC group. A correlation between QSM and plasma Al concentration was not found.

* Guarantor and correspondent: Y. Tan, Department of Radiology, First Clinical Medical Hospital, Shanxi Medical University, 85 Jiefang South Road, Taiyuan 030001, Shanxi Province, China.
** Guarantor and correspondent: H. Zhang, Department of Radiology, First Clinical Medical Hospital, Shanxi Medical University, 85 Jiefang South Road, Taiyuan 030001, Shanxi Province. China.
E-mail addresses: zhanghui_mr@163.com (H. Zhang), tanyan123456@sina.com (Y. Tan).
† These authors contributed equally to this work.

https://doi.org/10.1016/j.crad.2022.06.007
0009-9260/

Introduction

Mild cognitive impairment (MCI) refers to the clinical state in which a subject is cognitively impaired usually in the memory domain, but not diagnosed with dementia.[1] It has been estimated that 10–20% of individuals >65 years of age will be diagnosed as having MCI.[2] Studies[3,4] have shown that there is a higher annual rate of progression to Alzheimer's disease (AD) in those with MCI than that among the general population. Not all MCI patients will progress to AD and not all are progressive.[5] MCI can remain stable and a meta-analysis found that the reversal rate of up to 18% from MCI to normal cognition in the follow-up.[6] Therefore, early detection will enable treatment of symptoms, prevent MCI from progressing to AD, and improve quality of life.

Aluminium (Al) is one of the most prominent elements on Earth and it has been used in many aspects of life.[7] It can enter body from the skin, nasal cavity, lung, and gastrointestinal tract, and according to literature,[8] the inhalation route dominates. With regard to occupational workers, they could be exposed to Al mainly in metal processing industries. Reports[9,10] have shown Al has neurotoxicity and it is a potential risk factor for neurodegenerative diseases including MCI and AD. Al overload in the body can affect cell function and cause neuronal cell apoptosis, which eventually leads to cognitive decline.[11] Therefore, long-term exposure to Al will be harmful to the cognitive function of workers and cause MCI.

Recently, neuroimaging, in particular magnetic resonance imaging (MRI), has contributed to the identification of MCI. Susceptibility-weighted imaging (SWI) provides a feasible non-invasive method for investigating neurodegenerative diseases.[12] Gao *et al.*[13] found that the phase values of the caudate nucleus, red nucleus, and other areas in the MCI group and AD group were lower than that of control group. Kirsch *et al.*[14] reported that MCI patients who developed AD had significant iron deposition in the left putamen compared with other groups. These indicate that SWI can be applied to diagnose MCI and monitor whether MCI has progressed to AD; however, as the field strength changes caused by magnetic susceptibility are non-local, it is difficult to observe the tissue magnetic susceptibility distribution directly, and SWI cannot accurately reflect the local magnetic susceptibility changes of the tissue.[15] Thus, a more effective and highly sensitive biomarker is required to investigate MCI.

Quantitative susceptibility mapping (QSM) is a novel MRI post-processing technique based on SWI, which allows quantification of the spatial distribution of tissue magnetic susceptibility in vivo. It can show various complex organisational structures more clearly than SWI,[16–18] and it has been used to assess brain iron deposition in central nervous system diseases.[19,20] There have been only a few studies applying QSM to study MCI and the results are inconsistent.[21,22] Current research on QSM in diagnosing MCI in Al workers is even rarer. As Al and iron have similar chemical and physical properties, studies have shown that in AD patients, Al and iron levels in neuronal nuclei were markedly higher in AD brains than in age-matched control brains. Al and iron were found to co-localise in the nuclei of nerve cells, which might play a pivotal role in neuron degeneration and AD pathogenesis.[37] It was speculated that QSM could be used to diagnose MCI of occupational Al workers. Therefore, the aim of the present study was to explore the diagnostic value of QSM in MCI of Al workers, and analyse the correlation between QSM values, Montreal cognitive assessment (MoCA) scores, and plasma Al concentration, providing new ideas for early determination of MCI and assessment of the severity of cognitive decline.

Materials and methods

Subjects

This study is based on previous cohort studies.[36] This study was performed in a large-scale Al factory from October 2014 to November 2019. The basic characteristics, MoCA scores, plasma Al concentration, and MRI data of 60 occupational Al exposure workers were analysed retrospectively. Among them, seven subjects were excluded because of unclear QSM images (n=3), incomplete scanning of QSM image (n=1), and abnormal neuropsychological findings (n=3). After exclusions, 53 workers were included and divided into two groups. All subjects were male, with a median age of 48 (37–57) years old. The above-mentioned workers all wore work clothes and safety protection equipment at work. All participants voluntarily participated and signed an informed consent form. The study was approved by the Ethics and Human Committees of Shanxi Medical University. The results of MoCA scores (a total of 30 points) were evaluated by a senior physician.

Inclusion criteria for the study were as follows: (1) MCI group: a history of cognitive decline, MoCA score <26 points, complete and clear imaging data; (2) normal control group (NC group, 25 cases): gender, age and education level matched to the MCI group, MoCA score ≥26 points, complete and clear imaging data.

Exclusion criteria for the study were as follows: (1) any conditions that may cause cognitive impairment, including hepatic or renal disorders, brain trauma, cerebrovascular diseases, epilepsy, Parkinson's disease, and mental diseases; (2) any family history of dementia among first-degree relatives, such as AD; (3) any history of continuous medication with drugs containing Al, such as anti-acids or drugs affecting the central nervous system; (4) excessive smokers and alcoholics; (5) severe mental stimulation and shock in recent months (such as widowhood, death of parents or children, car accidents of oneself, parents or children, serious illness, property damage and disputes with others); (6) long-term consumption of Al-containing food such as excessive preference for vermicelli, fried dough sticks, and tea-containing drinks (>7 times/week); (7) engagement in Al-related work was <1 year; (8) with known poor vision and hearing; (9) unable to cooperate.

Determination of plasma Al concentrations

Approximately 10 ml of venous blood from each participant was collected, centrifuged in a centrifuge (4°C, 5 min, 1000 rpm), and the upper plasma was placed in a centrifuge tube. The experimental equipment, such as centrifuge tubes and pipette tips, should be soaked in acid for 3 days before use, and washed thoroughly and dried with an ultrapure water preparation device. The samples were transported to the laboratory and stored at −80°C until analysis. Plasma (0.4 ml) and 1.6 ml nitric acid (4%) were mixed well at room temperature for nitrification for 24 h, and the samples were subsequently analysed using inductively coupled plasma-mass spectrometry (ICP-MS) to measure plasma Al concentration. When measuring the sample, according to the random principle, the same sample was measured twice.

Image acquisition

MRI was acquired using a 3 T MRI system (Siemens) equipped with an eight-channel sensitivity encoding head coil. The scanning sequences included: T2-weighted imaging (T2WI), T2-weighted fluid-attenuated inversion recovery (T2FLAIR), three-dimensional high-resolution T1-weighted imaging (3D-T1WI), diffusion-weighted imaging (DWI), and QSM. According to T2FLAIR and 3D-T1WI images, malformations were excluded. The specific parameters of each MRI sequence were as follows: (1) T2WI: 3,570 ms repetition time (TR), 175 ms echo time (TE), 90° flip angle (FA), 6 mm thickness, 220 × 220 matrix, 220 × 220 mm field-of-view (FOV), 57 seconds acquisition time (TA); (2) T2FLAIR: 8,000 ms TR, 103 ms TE, 150° FA, 6 mm thickness, 220 × 220 matrix, 220 × 220 mm FOV, 144 seconds TA; (3) 3D-T1WI: 2,530 ms TR, 2.01 ms TE, 900 ms inversion time (TI), number of excitation (NEX) = 1, 7° FA, 256 × 256 mm FOV, 256 × 256 matrix, 1 × 1 × 1 mm voxel size, 1 mm thickness, 362 seconds TA; (4) DWI: 4,500 ms TR, 86 ms TE, 6 mm thickness, 220 × 220 mm FOV, 45 seconds TA. (5) QSM: 35 ms TR, 8.91, 14.58, 18.75, 22.92, 27.09, 31.26, 35.43, 39.6 ms TE, NEX = 1, 20° FA, 222.1 × 222.1 mm FOV, 294 × 352 matrix, 0.68 × 0.68 × 2.20 mm^3 acquisition voxel size, 402 seconds TA.

Post-processing of QSM

First, the original QSM data were exported in DICOM format. The MATLAB software package was used to process the image on the MRI post-processing workstation to obtain the QSM phase map fitted to different echoes. The steps of algorithm reconstruction included: (1) removal of the interference of the background magnetic field using the Projection onto Dipole Fields algorithm (PDF); (2) the inverse problem was solved based on the dipole by using the Morphology Enabled Dipole Inversion (MEDI) method to obtain the field pattern information related to the magnetic susceptibility of the tissue; (3) the ill-posed inverse problem was solved. The “dcm2niigui” software of the “MRIcroN” software package was used to convert the QSM data into “nii” format. After preprocessing, such as eddy current correction, Gaussian smoothing, and noise reduction, the nii format data were compressed to obtain the QSM map.

Parameter measurement

The regions of interest (ROIs) included the bilateral caudate nucleus, putamen, globus pallidus, thalamus, red nucleus, substantia nigra, dentate nucleus, hippocampus, genu of corpus callosum, splenium of corpus callosum, the cingulate gyrus, frontal white matter, parietal white matter, and temporal white matter (Electronic Supplementary Material Fig. S1).

MRIcroN software was used to adjust the contrast of the QSM map to clarify the boundaries of the ROIs and select the “view tool” for measurement. With T2 FLAIR and 3D-T1WI as the reference, the corresponding position on the QSM map was selected, and the symmetrical positions were selected on both sides. Then the ROIs were outlined manually and the susceptibility value was measured. The ROIs were drawn on consecutive optimal levels. In order to reduce error, they were measured three times by two experienced MRI physicians and the average value was taken as the final result. (1) The caudate nucleus head, putamen, globus pallidus, thalamus, red nucleus, substantia nigra, and dentate nucleus were measured according to their anatomical structure and high signal caused by the iron bipolar effect was avoided at the periphery of the nucleus and the edge was drawn along the inner side as shown on QSM; (2) the remaining ROIs were round with a diameter of 0.5 cm. When drawing ROIs, artefacts due to cerebrospinal fluid, blood vessels, and partial volume effects were avoided.

Statistical analysis

All data were analysed using SPSS V.22.0. If the experimental results of each group conformed to normal distribution and the variances were uniform, independent samples *t*-tests were conducted to test if these areas and the QSM values obtained from the MCI group and NC group were significantly different. On the contrary, a non-parametric test was used. Spearman’s correlation was used for correlation analysis between QSM values, MoCA scores, and plasma Al concentrations. A *p*-value of <0.05 was considered to be statistically significant. Finally, receiver operating characteristic (ROC) curve analysis was performed to show accuracy, sensitivity, and specificity. MedCalc software was used to compare differences in the area under the ROC curve (AUC) by *z* tests.

Results

Subject characteristics

Data from 53 Al factory workers were collected and all participates were male, with an age range of 37–57 years. The two groups did not differ significantly in age, gender, or education level. The plasma Al concentration of the MCI group was higher than that of NC, and the *p*-value has a

clear tendency to significance (p=0.057), which is summarised in Table 1.

Comparison of QSM values between the MCI group and NC group

Compared to the NC group, QSM values of left hippocampus, left dentate nucleus, right substantia nigra, and left putamen in the MCI group increased significantly (p<0.05). No significant differences were observed for other measured ROIs (p>0.05). The comparison results of QSM values are summarised in Table 2. Representative maps of patients in the MCI group and NC group are shown in Electronic Supplementary Material Figs. S2–3.

Correlation analysis

Spearman's correlation analysis showed that the QSM values of the left hippocampus, left dentate nucleus, right substantia nigra, and left putamen correlated negatively with MoCA scores (r=−0.610, p<0.001; r=−0.308, p=0.025; r=−0.391, p=0.004; r=−0.366, p=0.007, Table 3, Fig 1). It can be seen that with the decline of cognitive function, the magnetic susceptibility value in the brain of MCI patients gradually increases. No significant correlation was found between QSM values of the remaining ROIs and MoCA scores (p>0.05). No significant correlation was found between QSM values of all ROIs and plasma Al concentration (p>0.05, Table 4).

ROC curve analyses

The AUC of the left hippocampus, left dentate nucleus, right substantia nigra and left putamen were 0.907 (95% confidence interval [CI], 0.819–0.996), 0.693 (95% CI, 0.550–0.835), 0.743 (95% CI, 0.608–0.878), 0.700 (95% CI, 0.556–0.844), respectively. The accuracy, sensitivity and specificity were shown in Table 5.

The z test (Table 6, Fig 2) showed that the AUC of the left hippocampus was higher than that of other structures (p<0.05). The left hippocampus had higher accuracy, sensitivity, and specificity when distinguishing patients with MCI.

Table 1
Comparison of basic data in the mild cognitive impairment (MCI) group and normal controls (NC) group.

Items	MCI group	NC group	p-Value
No.	28	25	N.S.
Age (years)	47.39 ± 1.06	47.20 ± 0.97	0.90
Education[a] (years)	2.143 ± 0.12	2 ± 0.06	0.47
MoCA score	18.89 ± 0.46	27.96 ± 0.19	<0.001
Al (μg/l)	43.85 ± 4.91	33.10 ± 6.27	0.057

Data for age, education, MoCA score, and plasma Al concentration are presented as the mean ± standard deviation.
[a] Educational background 1 = primary school, 2 = junior high school, 3 = high school, 4 = university.

Table 2
Comparison of the difference of quantitative susceptibility mapping (QSM) values between the mild cognitive impairment (MCI) group and normal controls (NC) group ($\bar{x}$ ±s).

Regions of interest		MCI group (n=25)	NC group (n=25)	p-Value
Caudate nucleus	R	60.62 ± 4.23	57.17 ± 3.16	0.52
	L	60.03 ± 4.66	52.76 ± 3.45	0.23
Putamen	R	59.88 ± 4.83	66.60 ± 3.49	0.28
	L	70.00 ± 3.58	55.61 ± 4.00	0.010[a]
Globus pallidus	R	145.69 ± 6.41	148.07 ± 4.39	0.56
	L	146.78 ± 7.57	141.68 ± 5.67	0.60
Thalamus	R	-5.92 ± 2.31	-0.56 ± 1.95	0.090
	L	0.27 ± 2.28	0.96 ± 1.93	0.82
Substantia nigra	R	143.61 ± 6.60	114.11 ± 6.84	0.003[a]
	L	131.15 ± 7.71	134.28 ± 8.43	0.79
Red nucleus	R	115.26 ± 6.38	120.21 ± 6.41	0.59
	L	112.91 ± 7.15	123.57 ± 7.25	0.30
Hippocampus	R	-1.13 ± 4.01	-6.56 ± 4.62	0.21
	L	14.98 ± 2.90	-14.44 ± 3.09	<0.001[a]
Dentate nucleus	R	93.30 ± 6.50	91.46 ± 5.83	0.84
	L	106.70 ± 5.69	86.90 ± 4.67	0.016[a]
Frontal lobe	R	-13.18 ± 2.50	-11.57 ± 2.96	0.66
	L	-15.71 ± 2.09	-12.83 ± 2.13	0.34
Cingulate gyrus	R	-6.57 ± 3.64	-8.97 ± 3.59	0.64
	L	-2.58 ± 3.70	-8.60 ± 3.85	0.27
Temporal lobe	R	-8.29 ± 2.40	-10.13 ± 2.55	0.60
	L	-5.81 ± 2.90	-9.24 ± 3.10	0.42
Corpus callosum	Knee	-5.56 ± 2.89	-9.32 ± 3.08	0.38
	Genu	-6.56 ± 2.71	-9.56 ± 2.70	0.45
Parietal lobe	R	-5.98 ± 2.82	-9.37 ± 3.02	0.42
	L	-6.03 ± 2.80	-9.42 ± 3.00	0.41

The unit of QSM value is ppb ($\times 10^{-9}$).
R, right; L, left.
[a] These results indicate statistically significant differences.

Table 3
Correlation analysis between quantitative susceptibility mapping (QSM) values and Montreal Cognitive Assessment (MoCA) scores.

Regions of interest	MoCA score	
	p-Value	r-Value
Left hippocampus	<0.001	-0.61
Left dentate nucleus	0.025	-0.31
Right substantia nigra	0.004	-0.39
Left putamen	0.007	-0.37

p-Value is significant at 0.05 level (two-tailed).

Discussion

This study explored the diagnostic value of QSM in MCI of occupational Al workers, and analysed the correlation between QSM values, MoCA scores, and plasma Al concentration. This study found the QSM values of the left hippocampus, left dentate nucleus, right substantia nigra, and left putamen in the MCI group increased significantly, and left hippocampus had the best diagnostic efficacy. In addition, the QSM values correlated negatively with MoCA scores. No significant correlation was found between QSM values and plasma Al concentration.

MCI is usually described as an intermediate cognitive state between normal aging and dementia. It is reported that about 10–15% of MCI patients will progress to AD every year, while the incidence rate in the elderly age-matched

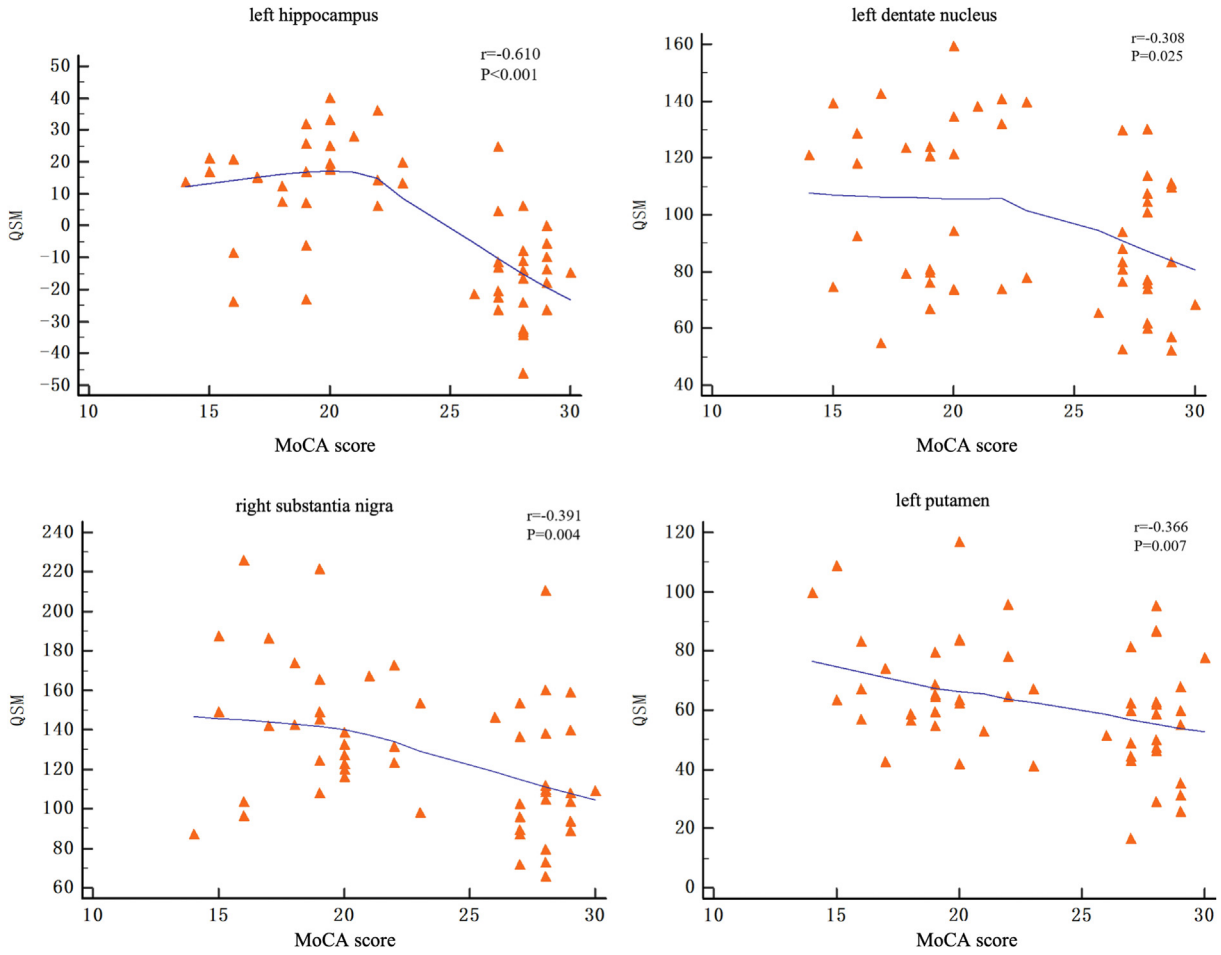

Figure 1 Correlation analysis of QSM values and MoCA scores of the left hippocampus (a), left dentate nucleus (b), right substantia nigra (c), and left putamen (d).

population is only 1–2%.[23,24] Moreover, the prevalence rate of MCI in retired Al pot-room workers (18.2%) was three-times greater than the NC group (5.7%).[25] Thus, Al workers represent a special group at high risk of progressing to cognitive decline. Accurate and timely interventions are the key to prevent the progression of MCI.[26]

The present study showed the left hippocampus had the best diagnostic efficacy compared with left dentate nucleus, right substantia nigra, and left putamen. This observation is similar to a previous study that showed that QSM values of the hippocampal fimbria was greater in patients with AD and can be detected at an early stage in AD[38]; however, Li *et al.*[39] found that the QSM values of the putamen were greater than the hippocampal values in the MCI and AD groups. This may be caused by the accumulation of non-paramagnetic material in different stages of AD, or it may be related to tissue structure.

The hippocampus is an advanced centre closely related to learning and memory, and is one of the most vulnerable areas in the brain of AD patients. A previous study showed that the cognitive function of retired Al workers declined after prolonged exposure to Al. Walton *et al.*[27] found that long-term exposure to Al would induce Al to accumulate in vital memory processing areas in mouse brains (such as the hippocampus). As a result, the level of amyloid precursor protein becomes elevated, causing the amyloid-β (Aβ) protein joint reaction to promote plaque formation and cause cognitive abnormalities. Mufson *et al.*[28] reported that Aβ plaques and neurofibrillary tangles (NFTs) deposited in the CA1 subregion of hippocampus at an early stage. The CA1 subregion is an area with the largest loss of hippocampal neurons in AD patients. It is responsible for transmitting information to the hippocampus, which is then transmitted to other cognitive structures to form a cognitive network. Hence, cognitive function will be damaged when the hippocampus has lesions. Kim *et al.*[29] found that the magnetic susceptibility had already changed during the MCI stage, and with progression of the disease, the susceptibility value of the hippocampus, thalamus, and many other parts gradually increased, suggesting that QSM can be used as an auxiliary imaging tool for assessing MCI. Hwang *et al.*[30] used QSM texture analysis to evaluate the change in texture characteristics with the progression of disease, and found that from the NC group to AD group, the QSM values showed a linear increasing trend. The present study found that QSM values correlated negatively with the MocA score. With impairment of cognitive function, the QSM values of MCI patients gradually increases, which is consistent with

Table 4
Correlation analysis between quantitative susceptibility mapping (QSM) values and plasma Al concentration.

Regions of interest		Plasma Al concentration (μg/l)	
		p-Value	*r*-Value
Caudate nucleus	R	0.773	-0.04
	L	0.571	-0.08
Putamen	R	0.244	-0.16
	L	0.236	-0.17
Globus pallidus	R	0.084	-0.24
	L	0.428	-0.11
Thalamus	R	0.417	-0.11
	L	0.198	-0.18
Substantia nigra	R	0.738	0.047
	L	0.111	-0.22
Red nucleus	R	0.538	-0.09
	L	0.645	-0.07
Hippocampus	R	0.804	0.035
	L	0.322	0.14
Dentate nucleus	R	0.330	-0.14
	L	0.975	-0.004
Frontal lobe	R	0.078	-0.24
	L	0.301	0.15
Cingulate gyrus	R	0.718	0.051
	L	0.521	0.090
Temporal lobe	R	0.423	0.11
	L	0.524	0.089
Corpus callosum	Knee	0.482	0.099
	Genu	0.475	0.10
Parietal lobe	R	0.492	0.096
	L	0.483	0.099

R=right; L=left.

the study of Zheng *et al.*[21] Moreover, the magnetic susceptibility value seems to clarify the severity of cognitive function impairment, so it is speculated that the QSM value of hippocampus may be a new imaging marker for evaluating the cognitive function of Al workers.

This study also found that the QSM values of the hippocampus, dentate nucleus, and putamen were slightly more significant on the left side, while the substantia nigra showed more obvious changes on the right side, indicating that the changes of magnetic susceptibility of bilateral hemispheres are not necessarily simultaneous. Other studies have also obtained the same results. Acosta-Cabronero *et al.*[31] found the magnetic susceptibility of right putamen in AD patients was slightly higher than that of the left, while the results of the study of Shuang *et al.*[32] were the opposite. Beard *et al.*[33] mentioned that iron could be transported along axons in dopaminergic neurons. Thus, the asymmetry of magnetic susceptibility values of the projected parts of dopaminergic neurons may be caused by the asymmetry of iron levels in the substantia nigra. As individuals have a dominant hemisphere and the processing activity and metabolism of the dominant hemisphere are greater than that of the other side, the distribution of magnetic substances may be affected, resulting in the asymmetry of susceptibility values of bilateral hemispheres.

Table 6
The comparison results of z test.

Pairwise comparison	z statistics	*p*-Value
Left hippocampus ~ left dentate nucleus	2.781	0.005
Left hippocampus ~ left putamen	2.468	0.014
Left hippocampus ~ right substanitia nigra	1.969	0.049
Left dentate nucleus ~ left putamen	0.075	0.94
Left dentate nucleus ~ right substantia nigra	0.488	0.63
Left putamen ~ right substantia nigra	0.418	0.68

The plasma Al concentration of the MCI group was higher than that of NC, and the *p*-value has a clear tendency to significance (p=0.057), and there was no correlation between QSM values and plasma Al concentration. This is different from the results of previous studies. Polizzi *et al.*[34] reported that the internal Al concentration of retired workers was almost twice that of the control group. A follow-up study by Rondeau *et al.*[35] showed that the Al concentration in drinking water would influence cognitive function. These indicate that the differences of individual variations such as Al intake and metabolism levels can cause different results. Although Al has neurotoxicity, for MCI workers who had been exposed to Al for a long time, the pathological mechanism does not seem to be related to plasma Al concentration and Al deposition in brain tissue. The changes in brain tissue of MCI patients are still between normal aging and AD, the pathological changes are so slight that it is difficult to identify clinically. Furthermore, the sample size of this study is relatively small, and plasma Al concentration of the sample fluctuates widely, which may affect the results of the study. Many researchers have reported that iron overload also participates in the pathogenesis of AD. Increased iron can be detected in Aβ protein and NFTs in the putamen and caudate nucleus of AD patients. Zheng *et al.*[21] found that iron accumulation was more likely to occur in the hippocampus, and the magnetic susceptibility values were negatively associated with cognitive scales. This provides a new basis for understanding the pathological mechanism of MCI. The QSM value measured in the present study is caused by Al overload or iron overload or the result of the combination of two metals, no definite conclusion could be drawn, the detailed mechanism remains to be further explored.

Table 5
ROC curve analysis results of quantitative susceptibility mapping (QSM) values in the mild cognitive impairment (MCI) group and normal controls (NC) group.

ROIs	The MCI group	NC group	AUC	Cut-off value	Accuracy (%)	Sensitivity (%)	Specificity (%)	*p*-Value
Left hippocampus	14.9837	-14.4431	0.907	6.8967	88.7	82.1	96.0	<0.001
Left dentate nucleus	106.6973	86.9015	0.693	116.1287	71.7	53.6	92.0	0.016
Right substantia nigra	143.6128	114.1169	0.743	114.4592	75.5	82.1	68.0	0.002
Left putamen	70.0051	55.6117	0.700	63.16	69.8	64.3	76.0	0.013

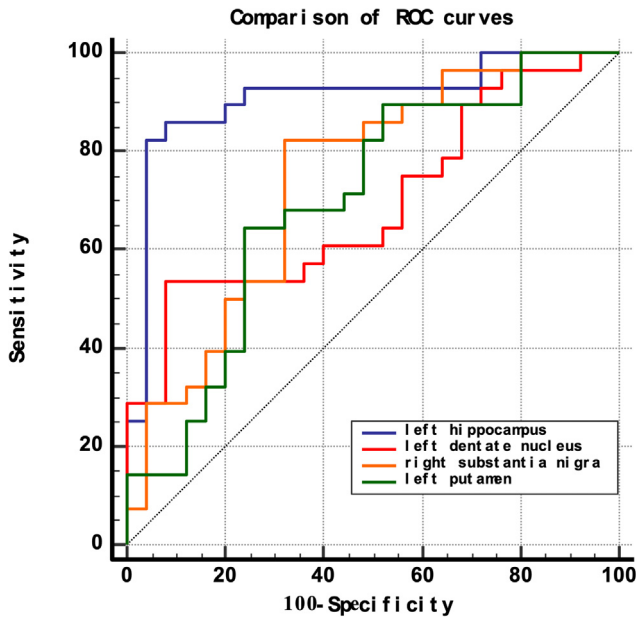

Figure 2 Comparison of ROC curves of QSM values of the left hippocampus, left dentate nucleus, right substantia nigra, and left putamen when discriminating the two groups.

This study has the following limitations: (1) the sample size was relatively small, and the subjects were all men. The results need to be expanded for further verification. (2) This study was a retrospective analysis, further longitudinal studies are needed to observe cognitive function dynamically. (3) The present study only investigated the distinguishing value of QSM in Al-exposed workers, and did not conduct joint analysis with other MRI technologies. Therefore, in the follow-up research, the sample size could be expanded, and multiple scales and other MRI techniques could be used in combination to further investigate the potential of QSM in the cognitive function of occupational Al workers.

In conclusion, QSM might be a reliable neuroimaging marker for the diagnosis of MCI. The left hippocampus showed the best diagnostic efficacy. The plasma Al concentration of the MCI group was higher than that of the NC group. A correlation between QSM parameters and plasma Al concentration was not found. The mechanism of damage remains to be elucidated fully.

Conflict of interest

The authors declare no conflict of interest.

Acknowledgements

The authors thank Shanxi Medical University, participants who took part in the study and those involved in data collection. This study was supported by the National Natural Science Foundation of China (81771824 and 81971593 to H.Z.; 81701681 and 82071893 to Y.T.; 81971592 to X.W.; the Precision Medicine Key Innovation Team Project (YT1601 to H.Z.); the Youth Innovation Fund (YC1426 to Y.T.); Fund Program for the Scientific Activities of Selected Returned Overseas Professionals in Shanxi Province (20200003 to Y.T.); the Youth Project of Applied Basic Research Project of Shanxi Province (201801D221403 to G.Y.); Science and Technology Innovation Project of University in Shanxi Province (2019L0440 to G.Y.).

Appendix A. Supplementary data

Supplementary data to this article can be found online at https://doi.org/10.1016/j.crad.2022.06.007.

References

1. Zhang Y, Chen X, Liang X, *et al.* Altered Weibull degree distribution in resting-state functional brain networks is associated with cognitive decline in mild cognitive impairment. *Front Aging Neurosci* 2020;**12**:599112, https://doi.org/10.3389/fnagi.2020.599112.
2. Petersen RC. Clinical practice. Mild cognitive impairment. *N Engl J Med* 2011 Jun 9;**364**(23):2227–34. https://doi.org/10.1056/NEJMcp0910237.
3. Anderson ND. State of the science on mild cognitive impairment (MCI). *CNS Spectr* 2019;**24**(1):78–87. https://doi.org/10.1017/S1092852918001347.
4. Mitchell AJ, Shiri-Feshki M. Rate of progression of mild cognitive impairment to dementia — meta-analysis of 41 robust inception cohort studies. *Acta Psychiatr Scand* 2009;**119**(4):252–65. https://doi.org/10.1111/j.1600-0447.2008.01326.x.
5. Weissberger G, Gibson K, Nguyen C, *et al.* Neuropsychological case report of MCI reversion at one-year follow-up. *Appl Neuropsychol Adult* 2018;**27**(3):284–93. https://doi.org/10.1080/23279095.2018.1519510.
6. Canevelli M, Grande G, Lacorte E, *et al.* Spontaneous reversion of mild cognitive impairment to normal cognition: a systematic review of literature and meta-analysis. *J Am Med Dir Assoc* 2016;**17**(10):943–8. https://doi.org/10.1016/j.jamda.2016.06.020.
7. Colomina MT, Peris-Sampedro F. Aluminum and Alzheimer's disease. *Adv Neurobiol* 2017;**18**:183–97. https://doi.org/10.1007/978-3-319-60189-2_9.
8. Exley C. Human exposure to aluminium. *Environ Sci Process Impacts* 2013;**15**(10):1807–16. https://doi.org/10.1039/c3em00374d.
9. Klotz K, Weistenhofer W, Neff F, *et al.* The health effects of aluminum exposure. *Dtsch Arztebl Int* 2017;**114**(39):653–9. https://doi.org/10.3238/arztebl.2017.0653.
10. Virk SA, Eslick GD. Occupational exposure to aluminum and Alzheimer disease: a meta-analysis. *J Occup Environ Med* 2015;**57**(8):893–6. https://doi.org/10.1097/JOM.0000000000000487.
11. Bagepally BS, Balachandar R, Kalahasthi R, *et al.* Association between aluminium exposure and cognitive functions: a systematic review and meta-analysis. *Chemosphere* 2021;**268**:128831, https://doi.org/10.1016/j.chemosphere.2020.128831.
12. Liu S, Buch S, Chen Y, *et al.* Susceptibility-weighted imaging: current status and future directions. *NMR Biomed* 2017;**30**(4), https://doi.org/10.1002/nbm.3552.
13. Gao L, Jiang Z, Cai Z, *et al.* Brain iron deposition analysis using susceptibility weighted imaging and its association with body iron level in patients with mild cognitive impairment. *Mol Med Rep* 2017;**16**(6):8209–15. https://doi.org/10.3892/mmr.2017.7668.
14. Kirsch W, McAuley G, Holshouser B, *et al.* Serial susceptibility weighted MRI measures brain iron and microbleeds in dementia. *J Alzheimers Dis* 2009;**17**(3):599–609. https://doi.org/10.3233/JAD-2009-1073.
15. Liu C, Li W, Tong KA, *et al.* Susceptibility-weighted imaging and quantitative susceptibility mapping in the brain. *J Magn Reson Imaging* 2015;**42**(1):23–41. https://doi.org/10.1002/jmri.24768.
16. Ippoliti M, Adams LC, Winfried B, *et al.* Quantitative susceptibility mapping across two clinical field strengths: contrast-to-noise ratio enhancement at 1.5T. *J Magn Reson Imaging* 2018;**48**(5):1410–20. https://doi.org/10.1002/jmri.26045.

17. Deistung A, Schweser F, Reichenbach JR. Overview of quantitative susceptibility mapping. *NMR Biomed* 2017;**30**(4), https://doi.org/10.1002/nbm.3569.
18. Haacke EM, Liu S, Buch S, *et al*. Quantitative susceptibility mapping: current status and future directions. *Magn Reson Imaging* 2015;**33**(1):1–25. https://doi.org/10.1016/j.mri.2014.09.004.
19. Wang Y, Spincemaille P, Liu Z, *et al*. Clinical quantitative susceptibility mapping (QSM): biometal imaging and its emerging roles in patient care. *J Magn Reson Imaging* 2017;**46**(4):951–71. https://doi.org/10.1002/jmri.25693.
20. Vinayagamani S, Sheelakumari R, Sabarish S, *et al*. Quantitative susceptibility mapping: technical considerations and clinical applications in neuroimaging. *J Magn Reson Imaging* 2021;**53**(1):23–37. https://doi.org/10.1002/jmri.27058.
21. Bo Z, Tianjing Z, Jiafei C, *et al*. Quantitative susceptibility mapping of the brain iron deposition in patients with mild cognitive impairment. *Int J Med Radiol* 2019;**42**(1):32–6. https://doi.org/10.19300/j.2019.L6218.
22. Yang Q, Zhou L, Liu C, *et al*. Brain iron deposition in type 2 diabetes mellitus with and without mild cognitive impairment—an in vivo susceptibility mapping study. *Brain Imaging Behav* 2018;**12**(5):1479–87. https://doi.org/10.1007/s11682-017-9815-7.
23. Langa KM, Levine DA. The diagnosis and management of mild cognitive impairment: a clinical review. *JAMA* 2014;**312**(23):2551–61. https://doi.org/10.1001/jama.2014.13806.
24. Vega JN, Newhouse PA. Mild cognitive impairment: diagnosis, longitudinal course, and emerging treatments. *Curr Psychiatry Rep* 2014;**16**(10):490. https://doi.org/10.1007/s11920-014-0490-8.
25. Lu X, Liang R, Jia Z, *et al*. Cognitive disorders and tau-protein expression among retired aluminum smelting workers. *J Occup Environ Med* 2014;**56**(2):155–60. https://doi.org/10.1097/JOM.0000000000000100.
26. Gauthier S, Reisberg B, Zaudig M, *et al*. Mild cognitive impairment. *Lancet* 2006;**367**(9518):1262–70. https://doi.org/10.1016/s0140-6736(06)68542-5.
27. Walton JR, Wang MX. APP expression, distribution and accumulation are altered by aluminum in a rodent model for Alzheimer's disease. *J Inorg Biochem* 2009;**103**(11):1548–54. https://doi.org/10.1016/j.jinorgbio.2009.07.027.
28. Mufson EJ, Binder L, Counts SE, *et al*. Mild cognitive impairment: pathology and mechanisms. *Acta Neuropathol* 2012;**123**(1):13–30. https://doi.org/10.1007/s00401-011-0884-1.
29. Kim H-G, Park S, Rhee HY, *et al*. Quantitative susceptibility mapping to evaluate the early stage of Alzheimer's disease. *NeuroImage: Clin* 2017;**16**:429–38. https://doi.org/10.1016/j.nicl.2017.08.019.
30. Hwang EJ, Kim HG, Kim D, *et al*. Texture analyses of quantitative susceptibility maps to differentiate Alzheimer's disease from cognitive normal and mild cognitive impairment. *Med Phys* 2016;**43**(8):4718. https://doi.org/10.1118/1.4958959.
31. Acosta-Cabronero J, Williams GB, Cardenas-Blanco A, *et al*. In vivo quantitative susceptibility mapping (QSM) in Alzheimer's disease. *PLoS One* 2013;**8**(11):e81093, https://doi.org/10.1371/journal.pone.0081093.
32. Shuang X, Chao C, Wen S, *et al*. Preliminary study of distribution and age-related changes of iron-content in the brain using MR quantitative susceptibility mapping. *Chin J Radiol* 2014;**48**(9):730–5. https://doi.org/10.3760/cma.j.issn.1005-1201.2014.09.008.
33. John B. Iron deficiency alters brain development and functioning. *J Nutr* 2003;**133**(Suppl. 1):1468S–72S. https://doi.org/10.1093/jn/133.5.1468S.
34. Polizzi SPE, Ferrara M, Bugiani M, *et al*. Neurotoxic effects of aluminium among foundry workers and Alzheimer's disease. *Neurotoxicology* 2002;**6**(23):761–74. https://doi.org/10.1016/S0161-813X(02)00097-9.
35. Rondeau V, Commenges D, Jacqmin-Gadda H, *et al*. Relation between aluminum concentrations in drinking water and Alzheimer's disease: an 8-year follow-up study. *Am J Epidemiol* 2000;**152**(1):59–66. https://doi.org/10.1093/aje/152.1.59.
36. Shang N, Zhang L, Wang S, *et al*. Increased aluminum and lithium and decreased zinc levels in plasma is related to cognitive impairment in workers at an aluminum factory in China: a cross-sectional study. *Ecotoxicol Environ Saf* 2021;**214**:112110, https://doi.org/10.1016/j.ecoenv.2021.112110.
37. Yumoto S, Kakimi S, Ishikawa A. Colocalization of aluminum and iron in nuclei of nerve cells in brains of patients with Alzheimer's disease. *J Alzheimers Dis* 2018;**65**(4):1267–81. https://doi.org/10.3233/JAD-171108.
38. Au CKF, Abrigo J, Liu C, *et al*. Quantitative susceptibility mapping of the hippocampal fimbria in Alzheimer's disease. *J Magn Reson Imaging* 2021 Jun;**53**(6):1823–32. https://doi.org/10.1002/jmri.27464.
39. Li D, Liu Y, Zeng X, *et al*. Quantitative study of the changes in cerebral blood flow and iron deposition during progression of Alzheimer's disease. *J Alzheimers Dis* 2020;**78**(1):439–52. https://doi.org/10.3233/JAD-200843.